



HAL
open science

Static and dynamic glass-glass transitions: a mean-field study

Luca Leuzzi

► **To cite this version:**

Luca Leuzzi. Static and dynamic glass-glass transitions: a mean-field study. *Philosophical Magazine*, 2008, 88 (33-35), pp.4015-4023. 10.1080/14786430802481911 . hal-00513978

HAL Id: hal-00513978

<https://hal.science/hal-00513978>

Submitted on 1 Sep 2010

HAL is a multi-disciplinary open access archive for the deposit and dissemination of scientific research documents, whether they are published or not. The documents may come from teaching and research institutions in France or abroad, or from public or private research centers.

L'archive ouverte pluridisciplinaire **HAL**, est destinée au dépôt et à la diffusion de documents scientifiques de niveau recherche, publiés ou non, émanant des établissements d'enseignement et de recherche français ou étrangers, des laboratoires publics ou privés.



Static and dynamic glass-glass transitions: a mean-field study

Journal:	<i>Philosophical Magazine & Philosophical Magazine Letters</i>
Manuscript ID:	TPHM-08-May-0167
Journal Selection:	Philosophical Magazine
Date Submitted by the Author:	15-May-2008
Complete List of Authors:	Leuzzi, Luca; INFN-CNR, SMC Center; University "Sapienza" of Rome, Dept. Physics
Keywords:	glass, statistical mechanics
Keywords (user supplied):	glass, statistical mechanics
<p>Note: The following files were submitted by the author for peer review, but cannot be converted to PDF. You must view these files (e.g. movies) online.</p> <p>submit_eps.tex stylefiles.tar</p>	



Philosophical Magazine

Vol. 00, No. 00, 00 Month 200x, 1–7

RESEARCH ARTICLE

Static and dynamic glass-glass transitions: a mean-field study

Luca Leuzzi

SMC Center, INFN-CNR and Dept. of Physics, University “Sapienza” of Rome,
P.le A. Moro 2, 00185, Rome, Italy

(Received 00 Month 200x; final version received 00 Month 200x)

The behavior of a family of mean-field glass models is reviewed. The models are analyzed by means of a Langevin-based approach to the dynamics and a Replica theory computation of the thermodynamics. We focus on the phase diagram of a particular model case, where glass-to-glass transitions occur between phases with a different number of characteristic time-scales for the relaxation processes. The appearance of Johari-Goldstein processes as collective reorganizations of sets of fast processes is discussed.

Theoretical modeling of glassy systems is a widespread topic. Different important theories have been introduced along the years like, e.g., the “free volume” [1], the “entropic” [2] and the “random first order” [3] theories, to mention a few. Nevertheless, a comprehensive theory both being analytically treatable and yielding reliable quantitative predictions above and below the glass transition has yet to be devised and appears to be a very complicated and challenging aim. In front of such limitations a theoretical approach based on the mean-field approximation, where statistical fluctuations of microscopic observables are neglected, helps pointing out a way to enforce realistic approaches and indentifying physically relevant concepts.

We present the study of a family of mean-field models with time-independent, i.e., *quenched*, disorder. The typical feature of amorphous systems is the impossibility to reach states at the lowest feasible energy, thus preventing crystallization. The system, undergoes some kind of “frustration”: because of dynamic arrest the global set of the energetic contributions due to the interactions among the glass former constituents cannot be simultaneously minimized. In the present case the frustration is a direct consequence of the quenched disorder. More generally it is self-generated by the inner geometry of the material and/or by the complicated exchange of interactions. The quenched disorder is not a necessary ingredient,¹ then, even though it makes the problem more easily tractable. The motivations for this study are manifolds. First, applying the replica method and using the concept of Replica Symmetry Breaking (RSB), the analysis of thermodynamic and dynamic properties can be carried out analytically. Then, it is possible to develop and check a multi-timescales equilibrium dynamics consistent at all times, including the asymptotic limit. Further, the model displays a very rich phase diagram with different glass and spin-glass phases, allowing for a theoretical analysis of the phenomenon

Email: luca.leuzzi@cnr.it, www.smc.infn.it

¹Glassy models without quenched disorder can be devised as well, see, e.g., Ref. [4].

ISSN: 1478-6435 print/ISSN 1478-6443 online
© 200x Taylor & Francis
DOI: 10.1080/1478643Yxxxxxxx
<http://www.informaworld.com>

Table 1. Phases and order parameters for models with quenched disorder.

PHASE	OVERLAP DISTRIBUTION
Paramagnet/Fluid	$P(q) = \delta(q)$
Glass	$P(q) = m\delta(q - q_0) + (1 - m)\delta(q - q_1)$
Spin-Glass*	$P(q) = w_0\delta(q - q_0) + \tilde{P}(q) + w_1\delta(q - q_1)$

* The function \tilde{P} is continuous on the support $]q_0 : q_1[$, w_0 and w_1 are weights of the δ 's ($w_0 + w_1 < 1$).

of polyamorphism.² Eventually, the identification of RSB's in the thermodynamics with time-scale separations in the dynamics [11] provides an useful theoretical tool to study the interrelation between primary (α), secondary (or Johari-Goldstein, β_{JG}) and tertiary processes (β_{fast} , γ). In this paper we will deepen the last two aspects and their possible implications for real structural glasses.

We first briefly introduce the model and sketch the computation of its thermodynamics within the Replica theory, emphasizing the nature of the order parameter and its change in behavior accross qualitatively different amorphous phases. The model Hamiltonian is:

$$\mathcal{H} = \sum_{i_1 < \dots < i_s} J_{i_1 \dots i_s}^{(s)} \sigma_{i_1} \dots \sigma_{i_s} + \sum_{i_1 < \dots < i_p} J_{i_1 \dots i_p}^{(p)} \sigma_{i_1} \dots \sigma_{i_p} \quad (1)$$

where $J_{i_1 \dots i_t}^{(t)}$ ($t = s, p$) are uncorrelated, zero mean, Gaussian variables of variance $J_t^2 t! / (2N^{t-1})$ and σ_i are N "spherical spins" obeying the constraint $\sum_i \sigma_i^2 = N$.

In a complex Free Energy Landscape (FEL), such as the one representing an amorphous system, the numerous valleys, i.e., the "glass states", can be more or less correlated among them and a hierarchy can be established based of their relative correlation.¹ Denoting by $\langle \dots \rangle_a$ the thermal average over the configurations belonging to state "a", the following *overlap* order parameter is defined as the correlation between two states (a and b):

$$q_{ab} = \frac{1}{N} \sum_{i=1}^N \langle \sigma_i \rangle_a \langle \sigma_i \rangle_b \quad (2)$$

To be precise, the complete order parameter is the *probability distribution* $P(q)$ of the values of q [14]. Depending on the shape of $P(q)$ one can identify a specific phase of the amorphous system. In table 1 we summarize the most common behaviors known in literature.

The replica theory for mean-field disordered systems is applied to compute the free energy functional [12, 13]:

$$-\beta\Phi = \frac{1}{2}(1 + \ln 2\pi) + \frac{1}{2} \lim_{n \rightarrow 0} \frac{1}{n} \sum_{ab}^{1,n} g(q_{ab}) + \ln \det \hat{\mathbf{q}} \quad (3)$$

where $\hat{\mathbf{q}} = \{q_{ab}\}$ is the Parisi overlap matrix. The model is specified by the function $g(q) \equiv q^s \mu_s / s + q^p \mu_p / p$, with $\mu_s = s\beta^2 J_s^2 / 2$. For a generic RSB Ansatz with R breakings the elements of the Parisi matrix take values $0 = q_0 < q_1 < \dots < q_R <$

²Many examples of polyamorphism are available in nature (and in literature). For example, the change in the kinetics of the coordination between molecules, occurring in vitreous Germania and Silica [5] or the sharp density change taking place in porous silicon [6], as well as in undercooled water [7]. Very recently polyamorphism in Ethanol [8], Laponite [9] and star polymer mixtures [10] has been observed.

¹A well known example is the symbolic dynamics through the Potential Energy Landascape, where intra-basin processes have a high correlation and inter-basin processes have a low correlation [16, 17].

1 $q_{R+1} = 1$ with relative multiplicities $n = m_0 > m_1 > \dots > m_R > m_{R+1} = 1$. As, in
 2 the Replica computation, $n \rightarrow 0$, the parameters m_r acquire real values ($\in [0, 1]$)
 3 [14] and one can express the set of q and m values as a (step) function $q(x)$.
 4 Here we are interested in structural glass. We will, thus, take into account model
 5 cases displaying phases with one and two step RSB, whose overlap functions are
 6 schematically represented on the left hand side of Fig. 1. These can be qualitatively
 7 connected with real glass formers in which only primary ($R = 1$) or also secondary
 8 ($R = 2$) processes are present.² Such glass models are realized taking $s > 2$ and
 9 large $p - s$ [20, 21]. Eq. (3) for a $R = 2$ RSB phase can be written as

$$-2\beta\Phi = 1 + \ln 2\pi + g(1) + m_2[g(q_2) - g(q_1)] + m_1[g(q_1) - g(q_0)] \quad (4)$$

$$+ \ln \chi_2 - \frac{1}{m_2} \ln \frac{\chi_2}{\chi_1} - \frac{1}{m_1} \ln \frac{\chi_1}{\chi_0} + \frac{q_0}{\chi_0} \quad (5)$$

12 with $\chi_2 = 1 - q_2$, $\chi_1 = \chi_2 + m_2(q_2 - q_1)$ and $\chi_0 = \chi_1 + m_1(q_1 - q_0)$.

13 In the $s + p$ models there are also different solutions (depending on the values of
 14 s and p and of T , J_s and J_p), displaying both continuous and discontinuous (and
 15 mixed) overlap functions. [12, 13].¹

16 The order parameter function (i.e., the set of values of m 's and q 's) is obtained
 17 by solving the following set of self-consistency equations:

$$g(q_2) - g(q_1) = (q_2 - q_1) \left[\Lambda(q_1) - \frac{1}{m_2 \chi_1} \right] - \frac{1}{m_2^2} \ln \frac{\chi_2}{\chi_1} \quad (6)$$

$$g(q_1) - g(q_0) = (q_1 - q_0) \left[\Lambda(q_0) - \frac{1}{m_1 \chi_0} \right] - \frac{1}{m_1^2} \ln \frac{\chi_1}{\chi_0} \quad (7)$$

$$\Lambda(q_0) = \frac{q_0}{\chi_0^2}; \quad \Lambda(q_1) - \Lambda(q_0) = \frac{q_1 - q_0}{\chi_0 \chi_1}; \quad \Lambda(q_2) - \Lambda(q_1) = \frac{q_2 - q_1}{\chi_1 \chi_2} \quad (8)$$

22 with $\Lambda(q) = dg(q)/dq$. The thermodynamics of the 1RSB solution is obtained from
 23 the above equations setting $q_2 = q_1$.

24 The value of the overlap corresponds to a given correlation among states, cf. Eq.
 25 (2). The three levels function displayed in the 2RSB solution corresponds to a pre-
 26 cise hierarchy in the organization of the thermodynamically relevant glassy states,
 27 consisting in groups of states (clusters) and groups of groups of states ("meta"-
 28 clusters). Two states whose overlap is q_2 belong to the same cluster. Two states
 29 whose overlap is q_1 do not belong to the same cluster but to the same meta-cluster.
 30 Eventually, two states whose overlap is q_0 (usually equal to zero in absence of ex-
 31 ternal forces of fields) belong to different meta-clusters.

32 The dynamics of the model is Langevin. Using a Martin-Siggia-Rose path-integral
 33 formalism one can reduce the equations of motion to a single variable formulation.
 34 Details can be found in Ref. [21]. The most important two-time observables are
 35 the correlation and response function

$$C(t, t_w) = \overline{\langle \sigma(t) \sigma(t') \rangle}; \quad G(t, t_w) = \frac{\delta \langle \sigma(t) \rangle}{\delta \beta h(t')} \quad t \geq t_w \quad (9)$$

36 Let us take an amorphous phase with a generic number $R (= 1, 2, \dots)$ of time-scale

56 ²From the point of view of Replica calculation we stress that a thermodynamically consistent example of
 57 a 2RSB phase has not been realized in models other than the $s + p$ spherical models [13].

58 ¹Usually, a glass phase is associated with discontinuous steps in the overlap, corresponding to a sharp
 59 separation of time-scales. A spin-glass phase is, instead, characterized by a fully continuous $q(x)$.

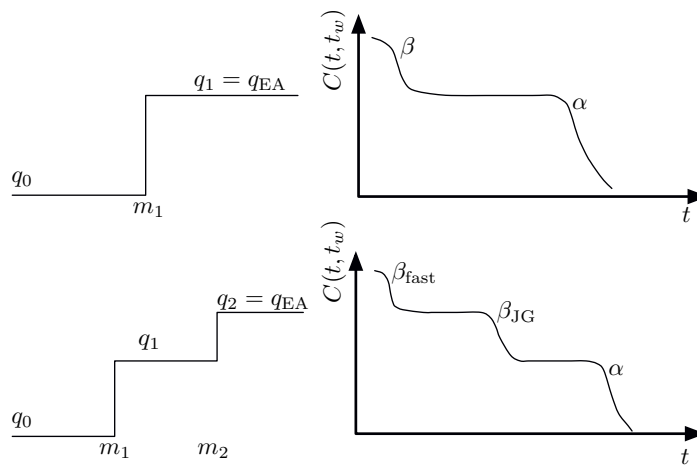


Figure 1. L.h.s.: order parameter step function $q(x)$ for the 1 and 2 RSB thermodynamic glassy phases. R.h.s.: Correlator vs. time for systems with processes relaxing on one and two well separated time-scales. A correspondence between the properties of the overlap function in the static solution and the behavior of the correlation function in the dynamics is shown (see also Eq. (12)).

bifurcations and assume that equilibrium is obtained in each (completely) disjoint time-sector, i.e. $t_w \rightarrow -\infty$. Using, e.g., a multiple scale analysis one assumes that the correlation function $C(t)$, as well as the response $G(t)$, can be represented as the sum of $R + 1$ distinct terms each depending on a time variable, $\tau_0 \ll \dots \tau_r \ll \dots \ll \tau_R$, describing the motion in a given time-sector:

$$C(t) = \sum_{r=0}^R C_r(\tau_r), \quad (10)$$

Considering a time-sector a means to probe the dynamics on times $t \sim \tau_a$. We can split off the a -sector function C_a taking the ordered limit

$$\widehat{\lim}_{t \rightarrow \infty} \equiv \lim_{\tau_R \rightarrow \infty} \dots \lim_{\tau_0 \rightarrow \infty}, \quad (11)$$

with the prescription $\tau_a/t = O(1)$, $\tau_{r < a}/t \rightarrow 0$ and $\tau_{r > a}/t \rightarrow \infty$. In practice, all contributions C_r to the correlation function with $r < a$ correspond to processes already thermalized at the observation time t , whereas all contributions whose index is larger than a represent processes that are frozen at time t . The interesting processes under probe are those *relaxing on characteristic times* $\tau_a \sim t$. In the above formulation, the asymptotic value of the correlator is, then, $C(t) \rightarrow q_r$, and we have the condition:

$$\widehat{\lim}_{t \rightarrow \infty} \left[\sum_{s=0}^{r-1} C_s(\tau_s) + \sum_{s=r}^R C_s(\tau_s) \right] = q_r \quad \forall r = 0, \dots, R \quad (12)$$

A schematic behavior of $C(t)$ for the cases of our interest, $R = 1, 2$, is plotted on the r.h.s. of Fig. 1, next to their overlap counterparts. In the top part we have the thermodynamic order parameter (step) function $q(x)$ displaying a single discontinuity at $x = m_1$. The two segments of the step function (q_0, q_1) can be linked, in the dynamics, to the two plateaus of the relaxation function in ordinary glass formers, in cases where secondary processes play no role. In the bottom part the 2RSB case is sketched, i.e., two discontinuities in $q(x)$ (thermodynamics), or two time-scale separations in C (dynamics). This is likely to be the mean-field

1 reduction of a glass with secondary processes.

2 The response function on multiple separated time-scales reads

$$3 \quad 4 \quad 5 \quad 6 \quad 7 \quad G(t) = \sum_{r=0}^R \frac{\tau_r}{t} G_r(\tau_r) \quad (13)$$

8 where each function G_r varies only in the corresponding sector r , $\tau_r \sim O(t)$ and
9 vanishes in all sectors with $s < r$. The function G_r represents the response of the
10 system to a perturbation in the time sector labeled by r , i.e., the response due to
11 all degrees of freedom which have not equilibrated in previous sectors.

12 Working with the Fourier transforms of the correlation and response functions
13 and defining the kinetic coefficient $\Gamma^{-1}(\omega) = i\partial_\omega G^{-1}(\omega)$, the dynamical stability
14 is guaranteed by the requirements $\Gamma(\omega_r) = 0, \forall r = 1, \dots, R$ and $\Gamma(\omega_0) > 0$, as the
15 ordered limit $\lim_{\omega_R \rightarrow 0} \dots \lim_{\omega_0 \rightarrow 0}$ is performed. In our $R = 2$ case the conditions
16 can be written as

$$17 \quad 18 \quad 19 \quad 20 \quad 21 \quad \Lambda'(q_2) = 1/\chi_2^2, \quad \Lambda'(q_1) = 1/\chi_1^2, \quad \Lambda'(q_0) > 1/\chi_0^2 \quad (14)$$

22 and provide the equations for the asymptotic dynamic solution. We stress that the
23 solution to Eq. (14) do not coincides with the static solution, Eqs. (6)-(8). This
24 is *typical of systems undergoing a dynamic arrest* before reaching a temperature
25 where they can undergo a thermodynamic phase transition. The thermodynamic
26 transition in these spin-glass inspired mean-field models for the glass is, instead,
27 the Kauzmann transition (at T_K), whereas the dynamic transition (at T_d) is equiv-
28 alent to the dynamic arrest transition predicted, e.g., in Mode Coupling Theory
29 (MCT). In real experiments it corresponds to the crossover temperature at which
30 the separation of time-scales of slow and fast processes accelerates.¹

31 A straightforward link with schematic models in MCT [18] can be drawn, start-
32 ing from the observation that the dynamic equations in random spherical models
33 are equivalent to the MCT equations [19] at high temperature, where time trans-
34 lational invariance (TTI) holds and G and C are connected by the fluctuation-
35 dissipation theorem (FDT), $G(t-t') = -\beta\theta(t-t')\partial_t C(t-t')$. In our model case,
36 thus, if we take a memory kernel depending on the correlator ϕ (in MCT notation)
37 as $m(\phi) = \mu_s\phi^{s-1} + \mu_p\phi^{p-1} = \Lambda(\phi)$, the mode coupling equations describe the
38 Langevin dynamics of the $s+p$ model and the overlap is identified with the non-
39 ergodicity parameter: $q = \lim_{t \rightarrow \infty} \phi(t)$. The two dynamics differ, instead, below
40 T_d , since the global TTI breaking is implicit in the random model dynamics, and
41 FDT does not apply anymore in the above form above.²

42 In mean-field models, unlike real glasses, the configurational entropy $S_c = \overline{\log \mathcal{N}_J}$
43 is a true state function. It can be formally computed as the Legendre transform of
44 the total free energy Φ , with f and βm as conjugated variables:

$$45 \quad 46 \quad 47 \quad 48 \quad 49 \quad 50 \quad S_c(f; T)/N = \min_m \left[-\beta m \Phi(m; T) - \beta m f \right] \quad (15)$$

51 where $m = m_R$. The configurational entropy of the thermodynamic solution is
52 subextensive ($S_c(f_{\text{eq}})/N \rightarrow 0, N \rightarrow \infty$, Kauzmann point). By maximizing S_c vs.

53
54
55
56
57
58
59
60
¹We notice that the experimental, calorimetric, glass temperature T_g is not defined in mean-field systems. Indeed, this is a property connected with the falling out of equilibrium of activated processes (hopping among valleys), whereas in mean-field metastable states are surrounded by infinite barriers (as $N \rightarrow \infty$). T_g lies, undetermined, between T_K and T_d .

²For details on the generalization of equilibrium dynamics in the solid amorphous phase see Ref. [21]).

6

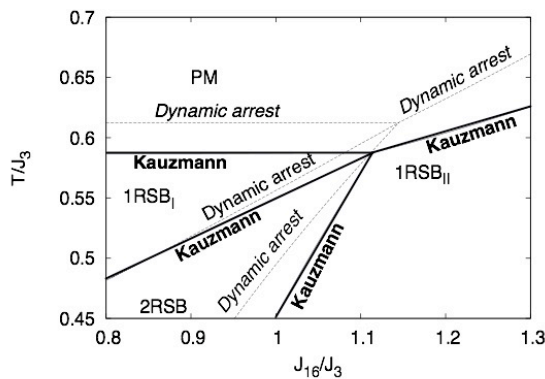


Figure 2. Phase diagram of the 3+16 model with both dynamic (dotted) and thermodynamic (full) transition lines. Four phases are present: paramagnetic (PM) at high T and three glass phases, here termed $1RSB_I$, $1RSB_{II}$ and 2RSB (see text).

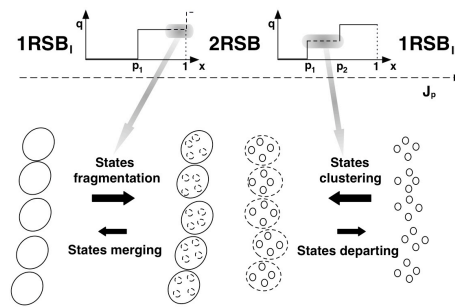


Figure 3. Interpretation of the GGT's in terms of metastable states organization. In one case a GGT occurs when fast processes slow down (and become secondary) and even faster processes appear (left, “states fragmentation”); in the other case secondary processes show up as new, intermediate, processes, between β_{fast} and α processes.

f , instead, we find the same values of q_r and m_r that solve the dynamic equations. As a consequence, *the dynamic arrest temperature can also be identified by looking at the temperature at which an extensive configurational entropy arise.*

In Fig. 2 we show a detail of the $(T/J_s, J_p/J_s)$ phase diagram of the $(s, p) = (3, 16)$ model around the tricritical point. Both dynamic and thermodynamic (i.e., Kauzmann) transition lines are plotted.¹ One can observe that decreasing T the dynamic transition between glass phases of different nature always precedes the thermodynamic one. The dynamic transition temperature $T_d(J_p)$ is the highest T at which the lifetime of high-lying local states becomes infinite and their number grows like $\exp(S_c(T))$ with the size N . The Kauzmann temperature $T_K(J_p)$ is, instead, the highest T at which $S_c(f_{eq})/N$ of the global *glassy*² minima goes to zero. The overlap order parameter jumps from 0 to q_{EA} while the free energy Φ is continuous: $\Phi_{liq}(T_K) = \Phi_{glass}(T_K)$.

At low T , two glass to glass transitions (GGT) occur, at the lower and higher J_p . We notice that they are not exactly of the same kind, in terms of local states hierarchy change. We schematically report in Fig. 3 how the states in the $1RSB$ phase reorganize as the system transforms into a 2RSB glass in the two cases. In the transition at low J_p a local state fragments into a cluster of new local states, whereas across the transition at high J_p subsets of uncorrelated local states group together in correlated clusters.

In conclusion, we have examined a mean-field model displaying, in particular, a phase whose thermodynamics is described by a 2RSB solution ($q(x) = q_0, q_1, q_2$). Recalling both the thermodynamic and the dynamic properties of this specific phase (including the GGT's from other glassy phases) and exploiting the equivalence between RSB's and time scale bifurcations, we argue that

- (1) changes connecting two local states in the same cluster of states ($q = q_2$) are β_{fast} (else called γ) processes,
- (2) changes connecting two local states in two different clusters belonging to the same cluster of clusters ($q = q_1$) correspond to JG processes,
- (3) changes connecting two uncorrelated states ($q = q_0 \approx 0$) contribute to the α relaxation.

¹The thermodynamic transition, termed “Kauzmann” in the figure, is a so-called “random first order transition”, with no latent heat but a discontinuous order parameter. This is an example of the mean-field scenario behind the mosaic theory [3]

²At higher temperature the global minima is a liquid/paramagnetic state.

1 The hierarchical nesting implicit in the present approach hints that fast processes
2 have a relevant influence on slow processes, even though taking place on well sepa-
3 rated time-scales. This very heuristic observation naturally stimulates a comparison
4 with Ngai's Coupling Model (see, e.g., Ref. [23] and references therein). A study
5 in this direction is in progress.
6
7
8

9 References

- 10
11 [1] D. Turnbull and M.H. Cohen, *J. Chem. Phys.* **34** (1961), 120.
12 [2] J.H. Gibbs and E.A. Di Marzio, *J. Chem. Phys.* **28** (1958), 373; AG. dam and J.H. Gibbs, *J. Chem.*
13 *Phys.* **43** (1965), 139.
14 [3] V. Lubchenko, P.G. Wolynes, *Ann. Rev. Phys. Chem.* **58** (2007), 235.
15 [4] E. Marinari, G. Parisi, F. Ritort, *J. Phys. A* **27** (1994), 7647; L. Cugliandolo et al., *Phys. Rev. Lett.*
16 **74** (1995), 1012; M. Mézard and G. Parisi, *Phys. Rev. Lett.* **82** (1999), 747.
17 [5] O.B. Tsiok et al., *Phys. Rev. Lett.* **80** (1998), 999. L. Huang and J. Kieffer, *Phys. Rev. B* **69** (2004),
18 224203. B. Champagnon et al., *J. Non-Cryst. Sol.* **353** (2007), 4208.
19 [6] S.K. Deb et al., *Nature* **414** (2001), 528.
20 [7] P.H. Poole et al., *Nature* **360** (1992), 324.
21 [8] V. Rodriguez-Mora and M.A. Ramos, *J. Non-Cryst. Sol.* **354** (2008).
22 [9] B. Ruzicka, L. Zulian, and G. Ruocco, *Phys. Rev. Lett.* **93**, 258301 (2004); *Langmuir* **22**, 1106 (2006).
23 [10] C. Mayer, *Phil. Mag.* present issue (2008).
24 [11] H. Sompolinsky, *Phys. Rev. Lett.* **47** (1981), 935.
25 [12] A. Crisanti and L. Leuzzi, *Phys. Rev. Lett.* **93**, 217203; *Phys. Rev. B* **73** (2006), 014412.
26 [13] A. Crisanti and L. Leuzzi, *Phys. Rev. B* **76** (2007), 184417.
27 [14] M. Mezard, G. Parisi, M. Virasoro, "Spin-glass theory and beyond", World Scientific, 1987.
28 [15] A. Crisanti, H. Horner and H.-J. Sommers, *Z. Phys. B* **92** (1993), 257.
29 [16] F. Sciortino, *J. Stat. Mech.* (2005) P05015.
30 [17] L. Leuzzi, T.M. Nieuwenhuizen, "Thermodynamics of the glassy state", Taylor & Francis, 2007.
31 [18] M. Fuchs *et al.*, *J. Phys.: Cond. Matt.* **3** (1991), 5047.
32 [19] J.-P. Bouchaud et al., *Physica A* **226** (1996), 243; S. Ciuchi and A. Crisanti, *Europhys. Lett.* **49**
33 (2000), 754.
34 [20] V. Krakoviack, *Phys. Rev. B* **76** (2007), 136401; A. Crisanti, L. Leuzzi, *ibid.*, 136402.
35 [21] A. Crisanti and L. Leuzzi, *Phys. Rev. B* **75** (2007), 144301.
36 [22] G.P. Johari and M.J. Goldstein, *J. Chem. Phys.* **53** (1970), 2372.
37 [23] K. L. Ngai, S. Capaccioli, *J. Phys: Cond. Matt.* **19** (2007), 205114.
38
39
40
41
42
43
44
45
46
47
48
49
50
51
52
53
54
55
56
57
58
59
60

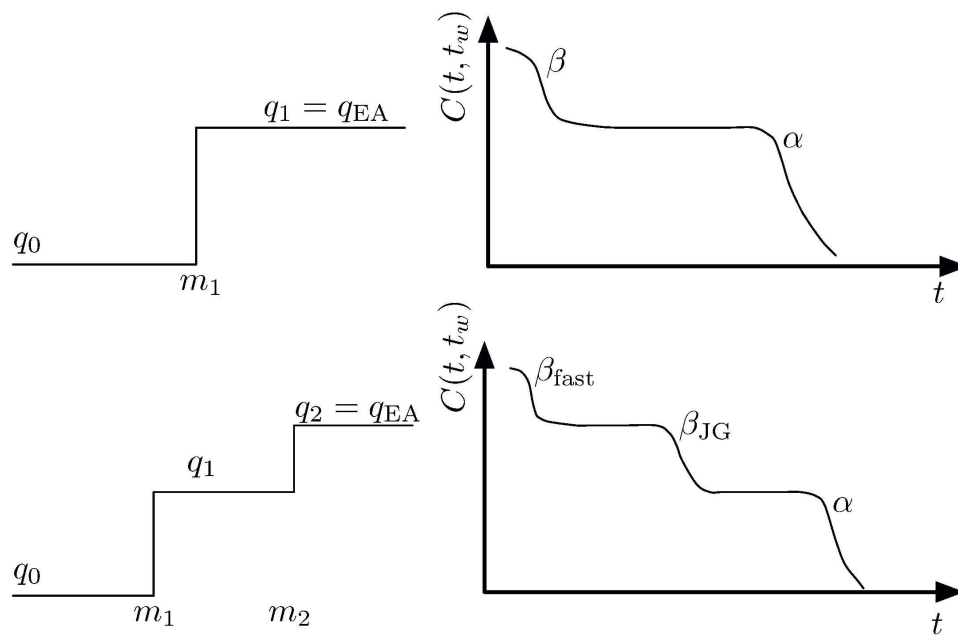


Figure 1
190x127mm (600 x 600 DPI)

Review Only

1
2
3
4
5
6
7
8
9
10
11
12
13
14
15
16
17
18
19
20
21
22
23
24
25
26
27
28
29
30
31
32
33
34
35
36
37
38
39
40
41
42
43
44
45
46
47
48
49
50
51
52
53
54
55
56
57
58
59
60

1
2
3
4
5
6
7
8
9
10
11
12
13
14
15
16
17
18
19
20
21
22
23
24
25
26
27
28
29
30
31
32
33
34
35
36
37
38
39
40
41
42
43
44
45
46
47
48
49
50
51
52
53
54
55
56
57
58
59
60

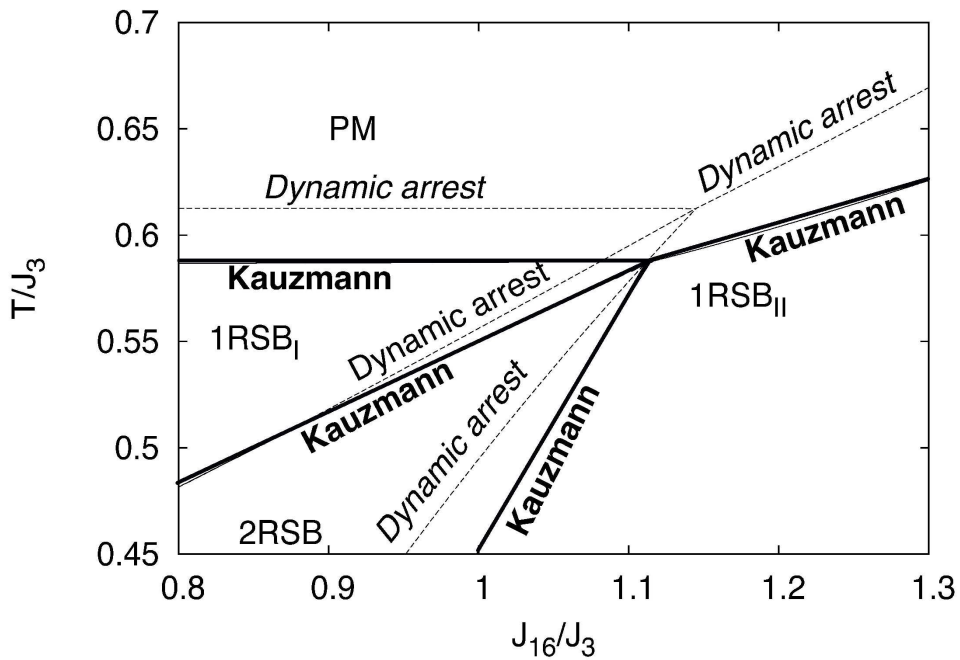


Figure 2
194x143mm (600 x 600 DPI)

Pre-proof Only

1
2
3
4
5
6
7
8
9
10
11
12
13
14
15
16
17
18
19
20
21
22
23
24
25
26
27
28
29
30
31
32
33
34
35
36
37
38
39
40
41
42
43
44
45
46
47
48
49
50
51
52
53
54
55
56
57
58
59
60

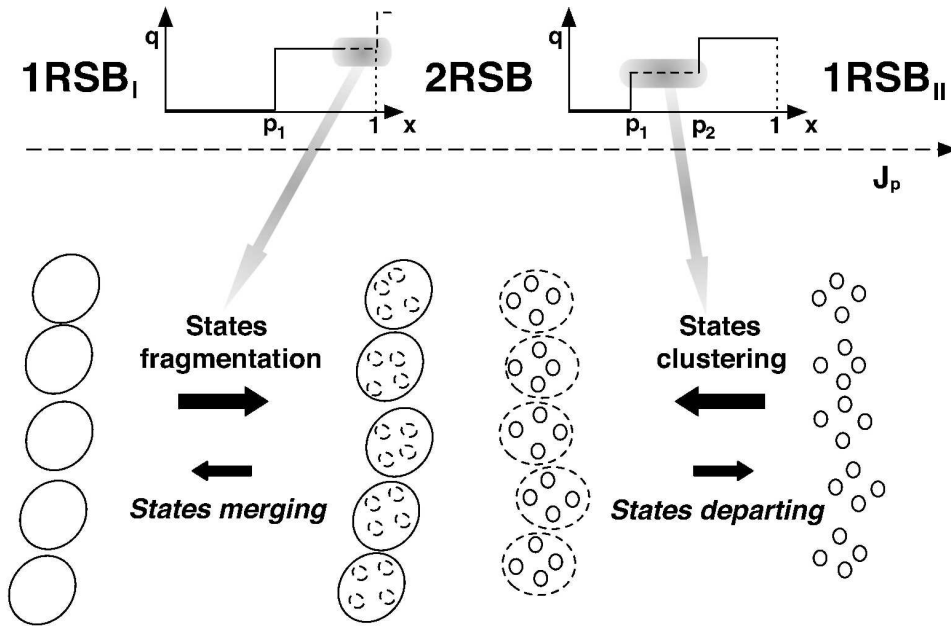


Figure 3
206x138mm (600 x 600 DPI)

view Only